Supplement
to
'*A Tandem Cell for Nanopore-based DNA Sequencing with Exonuclease*'

G. Sampath

This Supplement consists of the following sections and has some overlap with the main paper:

S-1 TANDEM CELL: PHYSICAL STRUCTURE

As noted in the main text, exonuclease sequencing[1] of DNA using a conventional cell is faced with a number of problems, which the tandem cell is designed to alleviate. A schematic of the tandem cell with two nanopores in tandem (Figure 1 in the main paper) is reproduced here as Figure S-1a. It has the structure [*cis*1, upstream nanopore (UNP), *trans*1=*cis*2, downstream nanopore (DNP), *trans*2]. A voltage difference V_{05} is applied between *cis*1 and *trans*2 using electrodes at the top of *cis*1 and the bottom of *trans*2, which results in a negatively charged strand of DNA being drawn from *cis*1 to and through UNP. An exonuclease enzyme covalently bonded to the downstream side of UNP cleaves the leading base from the DNA strand that has threaded through UNP. The negatively charged base moves toward DNP under the influence of the applied voltage and is detected as it passes through DNP where it is slowed down by a chemical adapter (biological DNP) or a profiled voltage (see Figure S-4 below, also Figure 4 in the main paper) applied over a segment of DNP (synthetic DNP). The voltage profile over the tandem cell that results from V_{05} is shown in Figure S-1b.

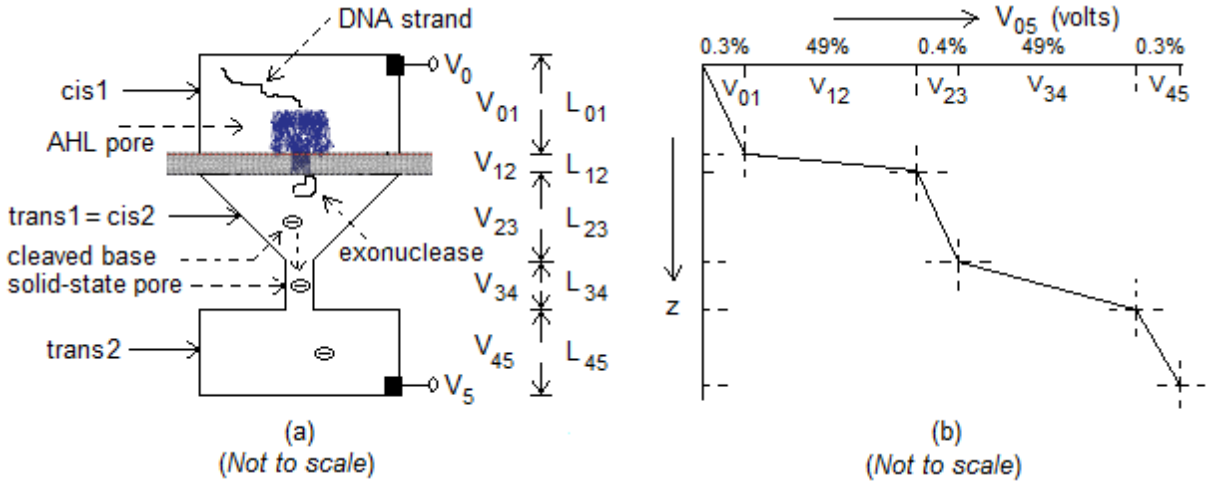

Figure S-1. Tandem cell with five pipelined stages: *cis*1, UNP (depicted here as an AHL pore), *trans*1= *cis*2, DNP (depicted here as a solid-state pore), and *trans*2. Dimensions considered: 1) *cis*1: box of height 1 μm, side 1 μm; 2) UNP: AHL pore of length 8-10 nm, diameter 2 nm; 3) *trans*1/*cis*2: tapered box of length 1 μm tapering from 1 μm^2 cross-section to 4 nm^2; 4) DNP: solid-state pore of length 10-20 nm and diameter 2 nm, or AHL pore as in UNP; 5) *trans*2: box of height 1 μm, side 1 μm. Electrodes assumed inserted at top of *cis*1 and bottom of *trans*2.

S-2 ANALYTICAL MODEL

The behavior of a cleaved base as it translocates through *trans*1/*cis*2 and DNP can be studied via the trajectory of a particle whose propagator function G(x,y,z,t) is given by a linear Fokker-Planck (F-P) equation in one or three dimensions. Such methods are commonly used in the study of translocation of biomolecules through a nanopore, see for example[2] and references therein. The F-P equation is used for piecewise analysis of the propagator in two sections: *trans*1/*cis*2 and DNP . Each section is modeled

independently in its own coordinate system and the transition occurring at the interface between the two stages studied separately. The coordinate systems used are shown in Figure S-2. Standard methods from partial differential equations and Laplace transforms are used.[3,4] The main quantity of interest here is φ(t), the pdf of the first passage time T (= the time for a cleaved base to translocate through the pore and be detected by the end of its translocation), which is independent of the coordinate system used.

S-3 TRANSLOCATION THROUGH DNP (*Detection*)

A one-dimensional approximation is applied to DNP (Figure S-2a: line segment $0 \le z \le L_{34}$; $t \ge 0$). A cleaved base is treated as a particle that is released at z = 0, t = 0; reflected at z = 0, t > 0; and captured at $z = L_{34}$, t > 0. The trajectory of the cleaved base as it passes through DNP is described by the function G(z,t) which satisfies

$$\partial G/\partial t + v_z\, \partial G/\partial z = D\, \partial^2 G/\partial z^2, \qquad z \in [0, L=L_{34}] \tag{1}$$

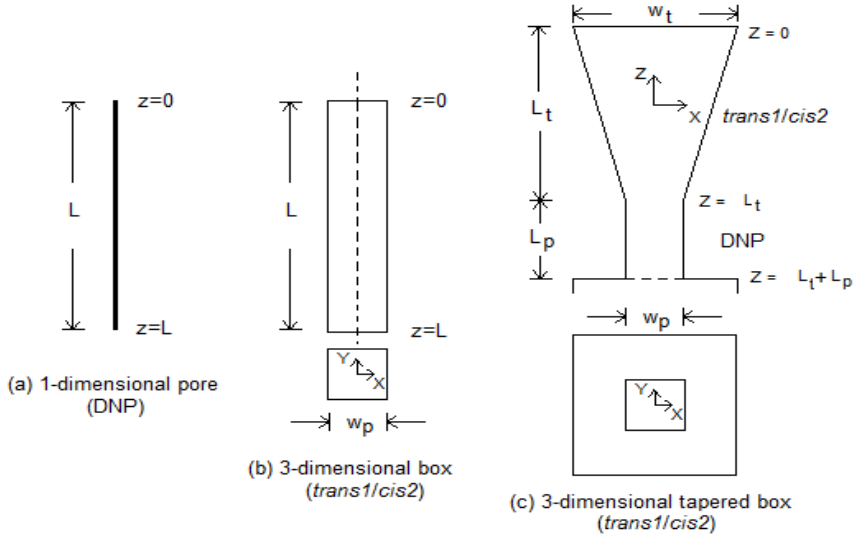

Figure S-2. Coordinate systems for different stages of the tandem cell (a) Stage 4, (b) Stage 3, (c) Stage 3. Dimensions used: (a) L= 8-10 nm; (b) L = 1 μm, w_p = 1 μm; (c) L_t = 1 μm, w_t = 1 μm, w_p = 2 nm.

with the following initial and boundary value conditions:

I.V. The particle is released at z = 0 and time t = 0:

$$G(0,t=0) = \delta(z) \tag{2}$$

B.C.1 The particle is captured at z = L:

$$G(L,t) = 0 \tag{3}$$

B.C.2 The particle is reflected at z = L:

$$D\, \partial G(z,t)/\partial z\,|_{z=0} = v_z\, G(z,t) \tag{4}$$

Here D is the diffusion constant and v_z, the drift velocity through DNP, is given by $v_z = \mu V_{34}/L$, where μ is the nucleotide mobility (assumed to be the same for all four base types). Following standard procedures φ(t), the pdf of the first passage time (translocation time) for a particle to diffuse-drift from z = 0 to z = L and get absorbed at z = L, can be obtained as

$$\varphi(t) = (2/(\sqrt{(\pi 4Dt^3)}\,[\, \textstyle\sum_{k=0}^{\infty} ((2k+1)L + v_z t) \exp(-((2k+1)L + v_z t)^2/(4Dt)) + \sum_{k=0}^{\infty} ((2k+1)L - v_z t) \exp(-((2k+1)L + v_z t)^2/(4Dt)) \tag{5}$$

φ(t) can be computed numerically but the series oscillates and converges very slowly. Therefore an alternative closed-form approach based on the earlier referenced model[2] of exonuclease-based sequencing is used. In that model a base is assumed to be cleaved above the pore of a conventional cell with the structure [*cis*, membrane-with-nanopore, *trans*] and drop into the pore. There is a non-zero probability of a cleaved base not entering the pore (given by a rate constant κ) and getting lost to diffusion. Setting κ to 0 in that model reduces it to the boundary value problem in Equations 1-4. Also the drift velocity v_z is not restricted to the downstream direction (*cis* to *trans*),[2] it can be positive or negative.
Modifying the main result in the earlier model,[2] the Laplace transform of the first passage time of a cleaved base passing through DNP is

$$\varphi^*(s) = \exp(\alpha/2) / [\cosh(y) + \alpha/2 \ \sinh(y)/y] \quad (6)$$

where

$$\alpha = v_z L/D; \qquad y^2 = \alpha^2/4 + 2\tau s; \qquad \tau = L^2/2D \quad (7)$$

The mean E(T) is

$$E(T) = -d\varphi^*(s)/ds\,|_{s=0} = (L^2/D\alpha)[1 - (1/\alpha)\,(1 - \exp(-\alpha))] \quad (8)$$

Similarly, the second moment $E(T^2)$ can be obtained as:

$$E(T^2) = d^2\varphi^*(s)/ds^2\,|_{s=0} = 2(L^2/D\alpha^2)^2(\alpha^2/2 + 3\alpha\exp(-\alpha) - 2 + \exp(-\alpha) + \exp(-2\alpha)) \quad (9)$$

From here the variance $\sigma^2(T) = E(T^2) - E^2(T)$ is obtained as

$$\sigma^2(T) = (L^2/D\alpha^2)^2\,(2\alpha + 4\alpha\exp(-\alpha) - 5 + 4\exp(-\alpha) + \exp(-2\alpha)) \quad (10)$$

where σ is the standard deviation.
For $v_z = 0$, these three statistics are given by

$$E_0(T) = L^2/2D; \qquad E_0(T^2) = (5/12)\,(L^4/D^2); \qquad \sigma_0^2(T) = (1/6)\,(L^4/D^2) \quad (11)$$

Figure S-3 shows the mean and standard deviation of T for different voltages across a DNP with L = 10 nm, $D = 3 \times 10^{-10}$ m^2/s, and $\mu = 2.4 \times 10^{-8}$ m^2/Vs.

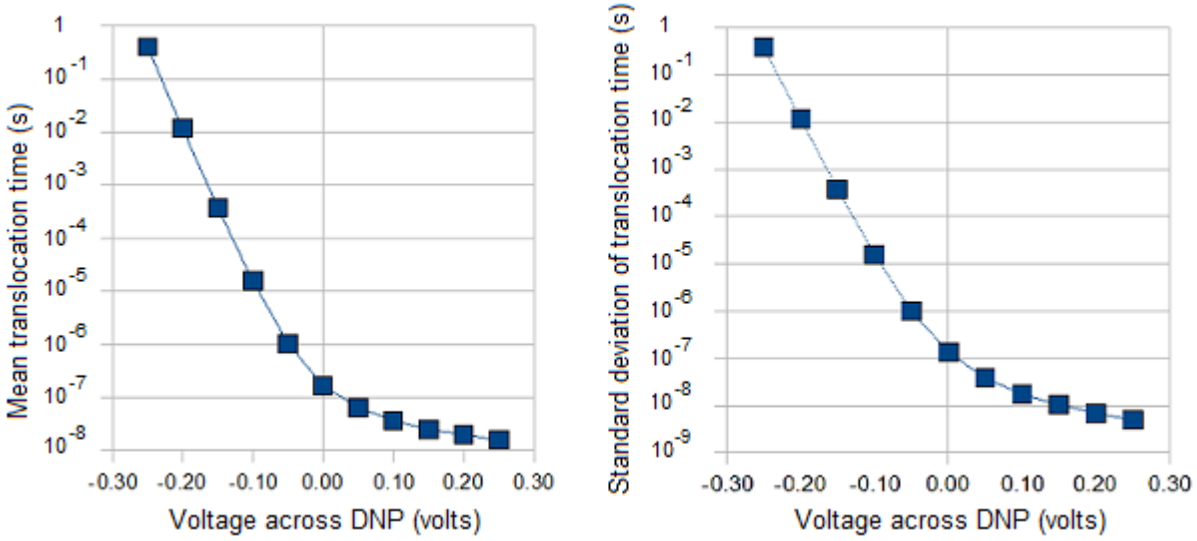

Figure S-3. Mean and standard deviation of time for particle to translocate from time of entry into DNP (negligible cross-section and length L = 8-10 nm) to time of exit into *trans*2. Parameter values used: mononucleotide mobility $\mu = 2.4 \times 10^{-8}$ m^2/Vs, diffusion constant $D = 3 \times 10^{-10}$ m^2/s. Calculations are for typical absolute potential difference in the range 0.1-0.3 V.

S-4 TRANSLOCATION THROUGH *trans*1/*cis*2 (*Delivery*)

For simplicity the *trans*1/*cis*2 compartment is assumed to be a rectangular box-shaped region (Figure 2b: box $0 \le z \le L_{23}$, $-d/2 \le x, y \le d/2$; $t \ge 0$). A particle is released at the top (0,0,0) at t = 0, reflected at the sides (x, y = ± d/2) and the top (z = 0) at t > 0, and translocates to the bottom ($z = L_{23}$) at t > 0, where it is 'absorbed'. 'Absorption' here means that the particle moves into DNP without regressing into *trans*1/*cis*2. Its behavior in DNP is described by the model pertaining to that section (see preceding analysis). The propagator function G(x,y,z,t) is given by a linear Fokker-Planck equation in three dimensions:

$$\partial G/\partial t + v_x\, \partial G/\partial x + v_y\, \partial G/\partial y + v_z\, \partial G/\partial z = D\,(\partial^2 G/\partial x^2 + \partial^2 G/\partial y^2 + \partial^2 G/\partial z^2) \tag{12}$$

where v_x, v_y, and v_z are the drift velocities in the x, y, and z directions, and D is the diffusion coefficient. In *trans*1/*cis*2 there is no drift potential in the x and y directions (Figure S-2b) so that

$$v_x = v_y = 0 \tag{13}$$

in Equation 12.

The following initial value (I.V.) and boundary values (B.C.) apply:

1) The particle is released at position (0,0,0) at time t = 0. This is represented by a delta function δ(x,y,z):

$$\text{I.V.} \qquad G(0,0,0,\, t=0) = \delta(x,y,z) = \delta(x)\,\delta(y)\,\delta(z) \tag{14}$$

2) It is reflected at the sides of *trans1*/*cis2* at t > 0:

$$\text{B.C. 1} \qquad D\,\partial G(x,y,z,t)/\partial x \,|_{\,x = \pm d/2} = 0 \tag{15}$$

$$\text{B.C. 2} \qquad D\,\partial G(x,y,z,t)/\partial y \,|_{\,y = \pm d/2} = 0 \tag{16}$$

3) It is reflected at the top of trans1/cis2:

$$\text{B.C. 3} \qquad D\,\partial G(x,y,z\,t)/\partial z \,|_{z\,=\,0} = v_z\, G(x,y,0,t), \quad t > 0 \tag{17}$$

4) It is absorbed at the bottom of *trans1*/*cis2* at t > 0:

$$\text{B.C. 4} \qquad G(x,y,L_{23}{=}L,t) = 0 \tag{18}$$

Since the initial value is a separable function of x, y, and z (Equation 14), the above boundary value problem in three dimensions can be considered mathematically as three boundary value problems,[3] one in each dimension, and the propagator function viewed as the product of three independent propagator functions:

$$G(x,y,z,t) = G_x(x,t)\, G_y(y,t)\, G_z(z,t) \tag{19}$$

where

$$G_x(x,t) = (2/d) \sum_{m=0}^{\infty} \cos \alpha_m x/\sqrt{D} \exp(-\alpha_m^2 t) \tag{20}$$

$$G_y(y,t) = (2/d) \sum_{n=0}^{\infty} \cos \beta_n x/\sqrt{D} \exp(-\beta_n^2 t) \tag{21}$$

and

$$G_z(z,t) = (2D/L) \exp(v_z z/2D + v_z^2/4Dt) \sum_{k=1}^{\infty} \sin \omega_k L \sin \omega_k (z-L) \exp(-D\omega_m^2 t\,)/N(\omega_k) \tag{22}$$

with

$$\alpha_m = 2m\pi\sqrt{D}/d \qquad \beta_n = 2n\pi\sqrt{D}/d \tag{23}$$

and

$$N(\omega_k) = (D/v_z)(\exp(v_z L/D)-1) - \{(v_z/D)(\exp(v_z L/D) - \cos 2\omega_k L) - 2\omega_k \sin 2\omega_k L)\}/((v_z/D)^2 + 4\omega_m^2) \tag{24}$$

If detection is defined to have occurred by the time the particle reaches z = L, the first passage time is the time the particle crosses z = L at any x and y, $-d/2 \le x,y \le d/2$, so that its pdf φ(t) can be written as

$$\varphi(t) = \int_{-d/2}^{d/2} \int_{-d/2}^{d/2} (-D\, dG(x,y,z,t)/dz\,|_{z=L})\, dx\, dy = \int_{-d/2}^{d/2} G_x(x,t)\, dx \int_{-d/2}^{d/2} G_y(y,t)\, dy\, \varphi_z(t) \quad (25)$$

where

$$\varphi_z(t) = 2D \exp(v_z z/2D - v_z^2/4Dt) \sum_{k=1}^{\infty} \omega_k \sin \omega_k L \exp(-D\omega_m^2 t)/N(\omega_k) \quad (26)$$

Similar to separation of the three-dimensional boundary value problem defined by Equations 12-18 into three independent one-dimensional boundary value problems, one can consider in physical terms a separation of diffusive effects in the three directions. With free diffusion given by Equations 12-13 and only the initial condition in Equation 14, the diffusion has a spatial mean of (0,0,0) and is independent in the three directions. Adding the reflective boundaries z = 0, x = ±d/2, and y = ±d/2 (see Figure S-1) and a positive drift potential ($V_{23} > 0$) causes the mean of the first passage time to z = L (which is an 'absorbing' boundary, where detection is considered to occur for any x and y; $-d/2 \le x,y \le d/2$) to be less than the mean time when $V_{23} = 0$. Considering $\varphi_z(t)$ in isolation, its distribution is in effect the one-dimensional first passage time distribution with mean $E(T = T_z)$ and standard deviation $\sigma = \sigma_z$.

To see if diffusion in the x and y directions has any effect on G(x,y,z,t) consider the factor $\int_{-d/2}^{d/2} G_x(x,t)\, dx$ in Equation 25 (the behavior of $G_v(y,t)$ is identical owing to the symmetry in x and y). To compute it the method of images[4] can be used. Thus start without any boundary conditions on x, which corresponds to free diffusion in x. $G_x(x,t)$ is given by the heat kernel:

$$G_x(x,t) = (1/(\sqrt{(\pi 4Dt)}) \exp(-x^2/(4Dt)), \qquad -\infty < x < \infty \quad (27)$$

This function is repeatedly reflected at x = ±d/2 resulting finally in

$$G_x(x,t) = (1/\sqrt{(\pi 4Dt)}[\exp(-x^2/4Dt) + \sum_{k=1}^{\infty} \exp(-(x+kd)^2/4Dt) + \sum_{k=1}^{\infty} \exp(-(x-kd)^2/4Dt)];\ -d/2 \le x \le d/2 \quad (28)$$

Because probability is conserved, the integral of $G_x(x,t)$ over $-d/2 \le x \le d/2$ is the area under the heat kernel function over $-\infty < x < \infty$, which is 1. A similar result holds for G(y,t) by symmetry. Hence Equation 25 reduces to

$$\varphi(t) = \varphi_z(t) \quad (29)$$

Thus diffusion in the x and y dimensions does not affect the translocation time distribution in the z direction (assuming of course that arrival of the particle at any (x,y,z=L) is tantamount to detection). Figure S-4 shows the dependence on pore voltage of the mean E(T) and standard deviation σ(T) of the translocation time through *trans*1/*cis*2 for L = 1 μm.

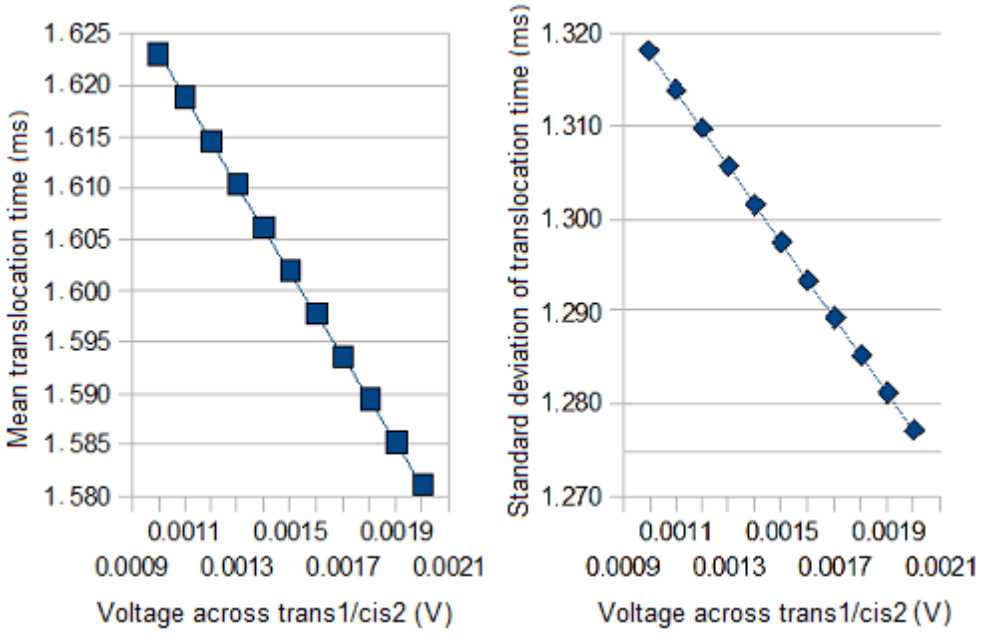

Figure S-4. Mean and standard deviation of translocation time for particle (cleaved base) released by exonuclease at top of *trans*1/*cis*2 (= 3-dimensional box with height 1 μm and cross-section 1 μm^2) to move to entrance of DNP. Parameter values used: mononucleotide mobility $\mu = 2.4 \times 10^{-8}$ m^2/Vs, diffusion constant $D = 3 \times 10^{-10}$ m^2/s. Calculations for cell voltages of 0.1-0.3 V, with ~1-2 mV dropping across *trans*1/*cis*2.

S-5 BEHAVIOR AT THE INTERFACE BETWEEN TWO SECTIONS

The Fokker-Planck model described above is a piecewise model that does not consider the behavior of the particle at the interface between two sections. In essence a particle jumps back and forth at the interface because of diffusion. This behavior can be studied by considering the probability currents at some fixed point on either side of the interface.

Consider the interface *trans*1/*cis*2-DNP at $(x,y,L_{23}\pm)$. If there is an absorbing barrier at L_{23}- then the probability function on the *trans*1/*cis*2 side would be

$$G_3(x,y,L_{23}-,t) = 0 \tag{30}$$

On the DNP side if there is a reflecting barrier the probability current would be

$$J_4(x,y,L_{23}+,t) = v_{z4}\, G_4(x,y,L_{23}+,t) - D\, \partial G_4(x,y,L_{23}+,t)/\partial z = 0 \tag{31}$$

$$v_{z3} = \mu V_{23}/L_{23} \qquad v_{z4} = \mu V_{34}/L_{34} \tag{32}$$

But there is really no barrier. The particle oscillates randomly at the interface before eventually passing into DNP, such passage being aided directly by the positively directed drift potentials in both compartments and indirectly by the reflecting boundaries in *trans*1/*cis*2. Thus

$$J_3(x,y,L_{23}-,t) = v_{z3}\, G_3(x,y,L_{23}-,t) - D\, \partial G_3(x,y,L_{23}-,t)/\partial z \neq 0 \tag{33}$$

and

$$J_4(x,y,L_{23}+,t) = v_{z4}\, G_4(x,y,L_{23}+,t) - D\, \partial G_4(x,y,L_{23}+,t)/\partial z \neq 0 \tag{34}$$

Continuity requires

$$J_3(x,y,L_{23}-,t) = J_4(x,y,L_{23}+,t) \tag{35}$$

In order for the particle to translocate successfully through DNP in the z direction so that it can be detected inside DNP, the net probability current at L_{23} must be in the positive z direction. This can be achieved with a sufficiently large V_{05}, as long as the resulting electric field is below the breakdown limit of ~70 MV/m (assuming 1 mole KCl for the electrolyte). Thus

$$J_{34}(x,y,L_{23},t) = J_3(x,y,L_{23}-,t) = J_4(x,y,L_{23}+,t) > 0 \tag{36}$$

The behavior at the interface between DNP and *trans*2 is similar.

The tapered geometry of *trans*1/*cis*2 in Figure S-1a aids drift of the particle into DNP. It can be modeled with a Fokker-Planck equation just as in Equation 12 but with a trapezoidal frustum boundary. The resulting system of equations is not as easily solved as Equations 12 through 18 although it is amenable to numerical solution. One obvious result is that the translocation time is decreased. Similar to the taper in *trans*1/*cis*2 aiding capture of the base at the entrance of DNP the abrupt increase in diameter from DNP to *trans*2 decreases the probability of a detected particle regressing into DNP from *trans*2. One can also think of these two behaviors in terms of entropy barriers[5]: the taper in *trans*1/*cis*2 decreases the barrier for entry into DNP (below what it would be with a rectangular box), while the step change going from DNP to *trans*2 effectively increases the barrier for a base trying to regress into DNP.

S-6 NEGATIVE FIELD OVER DNP

Let the electric fields over the five sections of the tandem cell be E_{01}, E_{12}, E_{23}, E_{34}, and E_{45}. Consider DNP in isolation. With a negative electric field E_{34} over DNP of length L_{34} = 10 nm, $D = 3 \times 10^{-10}$ m^2/s, and $\mu = 2.4 \times 10^{-8}$ m^2 /Vs, the data in Figure S-5 show an increase in the mean translocation time, which indicates slowdown, but it is also accompanied by a significant increase in the variance. With V_{34} approaching -0.25 V, the mean has increased by 7 orders of magnitude over the mean for V_{34} = 0.25 V, and the standard deviation is closely tracking the mean, indicating that diffusion has started to take over.

For this approach to work: 1) A cleaved base entering DNP must not regress into *trans*1/*cis*2; 2) A detected base exiting into *trans*2 must not regress into DNP; 3) The probability that there is more than one base in DNP must approach 0. To satisfy condition 1 a base moving from *trans*1/*cis*2 into DNP has to experience a positive drift field at the interface. This requires that E_{23} and E_{34} both be positive. To satisfy condition 2 a base moving from DNP into *trans*2 has to experience a positive drift field at the interface. This requires that E_{34} and E_{45} both be positive. Slowing down the base inside DNP requires E_{34} to be negative. All three field sign conditions may be satisfied if L_{34} is split into three parts $L_{34\text{-}0\ 34\text{-}1}$, $L_{34\text{-}1\ 34\text{-}2}$, and $L_{34\text{-}2\ 34\text{-}3}$ with respective electric fields $E_{34\text{-}0\ 34\text{-}1}$, $E_{34\text{-}1\ 34\text{-}2}$, and $E_{34\text{-}2\ 34\text{-}3}$ such that $E_{34\text{-}0\ 34\text{-}1} > 0$, $E_{34\text{-}1\ 34\text{-}2} < 0$, and $E_{34\text{-}2\ 34\text{-}3} > 0$. Such an electric field profile is shown in Figure S-5. (Condition 3 is examined later in this section and shown to be satisfied theoretically.)

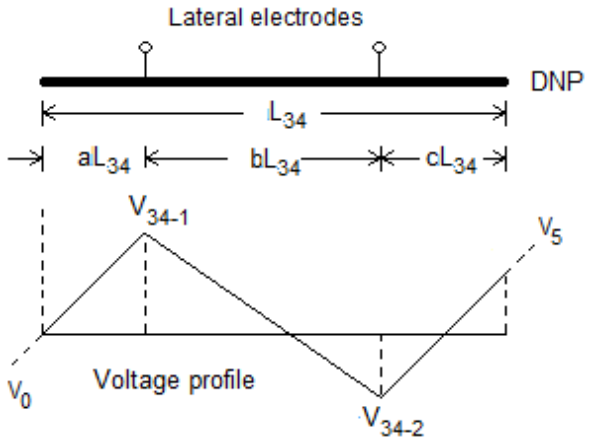

Figure S-5 Example of a profiled voltage over DNP in which the pore length is divided into three segments $L_{34\text{-}1}$, $L_{34\text{-}2}$, and $L_{34\text{-}3}$, with lengths $L_{34\text{-}1} + L_{34\text{-}2} + L_{34\text{-}3} = L_{34}$. Electric field is positive over $L_{34\text{-}1}$ and $L_{34\text{-}3}$, negative over $L_{34\text{-}2}$. (The voltages themselves need not be negative. Thus $V_{34\text{-}1} - V_{34\text{-}0} > 0$, $V_{34\text{-}3} - V_{34\text{-}2} > 0$, and $V_{34\text{-}2} - V_{34\text{-}1} < 0$.) Also $V_{34\text{-}0} > V_{23}$ (voltage across *trans*1/*cis*2) and $V_{34\text{-}3} < V_{45}$ (voltage across *trans*2).

The earlier model and analysis of DNP may be extended to the behavior of a base that experiences this kind of profiled potential when inside DNP. There is a tradeoff among the need to reduce the translocation speed through DNP, the need to prevent regression from DNP into *trans*1/*cis*2, and the need to prevent regression into DNP from *trans*2. Let $L_{34\text{-}0\ 34\text{-}1} = a\,L_{34}$, $L_{34\text{-}1\ 34\text{-}2} = bL_{34}$, and $L_{34\text{-}2\ 34\text{-}3} = cL_{34}$, with $a + b + c = 1$. The first and second conditions require $E_{34\text{-}0\ 34\text{-}1}$ and $E_{34\text{-}2\ 34\text{-}3}$ both to be sufficiently positive (see Equation 36 and associated discussion above). Since two electrodes are required to define the internal negative potential segment, each of a, b, and c has a minimum value given by $a_{min} = b_{min} = c_{min} = e_w + e_s$, where e_w = width of electrode

and e_s = interelectrode spacing. This spacing along with the applied voltages $V_{34\text{-}1}$ and $V_{34\text{-}2}$ can be used to determine the span of the negative electric field over DNP (Figure S-5). (The voltages themselves need not be negative, it is the potential difference, and hence the resulting electric field, that has to be negative.)

With this modification DNP can be represented as [Si pore, electrode, Si pore, electrode, Si pore]. It may be possible to achieve the desired field profile if ultra thin graphene sheets (which have been studied for their potential use in strand sequencing) are used for the electrodes. Figure S-6 shows a schematic of the required modification, where voltages are applied to electrodes V_0, $V_{34\text{-}1}$, $V_{34\text{-}2}$, and V_5. Voltage drops are assumed to be similar to those noted in the earlier referenced exonuclease model[2]. Thus 49% of the potential difference $V_{0\ 34\text{-}1}$ drops across each of UNP and the segment $L_{34\text{-}0\ 34\text{-}1}$ and 0.5% across each of *cis*1 and *trans*1/*cis*2. A negative electric field exists across the segment $L_{34\text{-}1\ 34\text{-}2}$ with $V_{34\text{-}1} > V_{34\text{-}2}$. With $V_4 > V_{34\text{-}2}$, 99% of the potential difference $V_{34\text{-}2\ 4}$ drops across the segment $L_{34\text{-}2\ 34\text{-}3}$ and 1% across *trans*2.

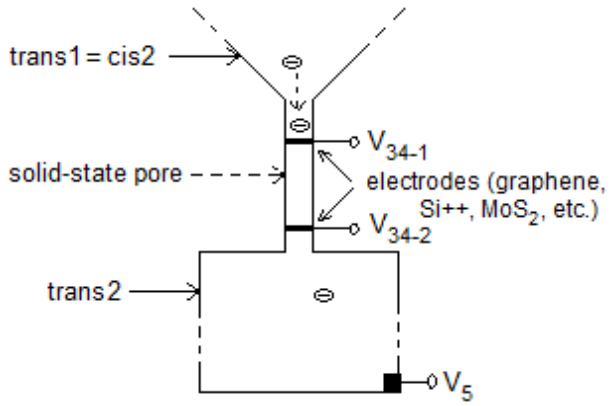

Figure S-6. Tandem cell modified for negative field over segment of DNP. Graphene electrodes laterally inserted into DNP. Negative field applied over middle segment of DNP through graphene electrodes set to voltages $V_{3\text{-}1}$ and $V_{3\text{-}2}$. Thus $V_0 < V_{3\text{-}1}$, $V_{3\text{-}2} < V_{3\text{-}1}$, $V_{3\text{-}2} < V_5$, where V_0 and V_5 represent electrodes in *cis*1 and *trans*2.

The optimum electric field profile over DNP can be obtained by experiment. Here an estimate is obtained by using Equations 8 and 10 from the one-dimensional problem while ignoring the transitional behavior at the two ends. Let $V_{34\text{-}0\ 34\text{-}1} = V_{34\text{-}1} - V_{34\text{-}0} = V_a$, $V_{34\text{-}1\ 34\text{-}2} = V_b$, and $V_{34\text{-}2\ 34\text{-}3} = V_c$. With $V_a = V_c = 0.05$ V and $V_b = -0.18$ V the mean and standard deviation of the translocation time over each of the three segments of a nanopore of length $L_{34} = 10$ nm are shown in Table S-1 for different values of a and b. The translocation over the segment $[aL_{34}, aL_{34} + bL_{34}]$ is seen to be considerably slowed down by the negative field, which also dominates the total translocation time over DNP.

Table S-1
Translocation times over positive and negative electric field segments of DNP

a = c (positive field segment)	Mean (10^{-8} s)	Standard deviation (10^{-8} s)	b (negative field segment)	Mean (10^{-3} s)	Standard deviation (10^{-3} s)
0.1	0.063	0.038	0.8	1.84574	1.84573
0.2	0.252	0.152	0.6	1.038229	1.038222
0.3	0.566	0.344	0.4	0.461435	0.461432
0.4	1.006	0.611	0.2	0.1153588	0.1153580

S-7 ADDITIONAL IMPLEMENTATION NOTES

Slowdown over a synthetic DNP using a negative field

Similar to graphene sheets, Si++ or molybdenum sulphide (MoS_2) layers with nanopores[6] may be used. A graphene/MoS_2 sheet with nanopore by itself can be used for exonuclease sequencing with a tandem cell. The cell structure would then be [*cis*1, UNP, *trans*1=*cis*2, DNP, *trans*2], where DNP is [Si pore, transverse electrode, Si pore, graphene/MoS_2 ribbon/sheet, Si pore, transverse electrode, Si pore]. The translocating cleaved base is identified by the level of the transverse current through the graphene/MoS_2 sheet. Negative fields may also be used in strand sequencing. The translocation speed can be controlled by embedding the graphene/MoS_2 layer in the negative-field segment of a solid-state nanopore with an electric field profile similar to that in Figure

S-5. A cell would then have the structure [*cis*, Si pore, transverse electrode, Si pore, graphene/MoS_2 ribbon/sheet, Si pore, transverse electrode, Si pore, *trans*], where the large thickness of the Si pore, by itself a disadvantage in strand sequencing, is no longer important. In both strand and exonuclease sequencing using the above approach, the μA-level transverse currents through a graphene or molybdenum disulphide sheet/nanoribbon plus the negative-field-based slowdown of strand or cleaved base could result in a lower detection bandwidth and S/N ratios that are significantly higher than with a method that relies only on axial ionic pore currents < 100 pA.

Slowdown over a biological DNP (AHL with adapter)

With AHL for DNP and a covalently attached cyclodextrin adapter used for slowdown, residence rates obtained from exonuclease sequencing experiments[1] require changes in some of the device parameters to satisfy the two conditions discussed in the main text. The first condition, namely that two successively cleaved bases stay in order when they enter DNP (Equation 1 in the main text) is

$$T > (\mu_{T1}+3\sigma_{T1}) - \max(0, \mu_{T2}-3\sigma_{T2}) \quad (37)$$

The second condition is the sufficient condition for two bases not being in the pore at the same time (Equation 2 in the main text):

$$T + \max(0,\mu_{T2}-3\sigma_{T2}) > \mu_{T1} + 3\sigma_{T1} + \mu_P + 3\sigma_P \quad (38)$$

where T is the interval (which is a random variable) between two successively cleaved bases 1 and 2. (That the second condition subsumes the first can be seen by comparing Equations 37 and 38.)

Assume two successive cleaving intervals T_1 and T_2 to be independent and identically distributed (i.i.d.). Let $\mu_{T1} = \mu_{T2}$ = mean translocation time through *trans*1/*cis*2, μ_P = mean translocation time of a base through DNP, and $\sigma_{T1} = \sigma_{T2}$ and σ_P the corresponding standard deviations. Experiments in exonuclease sequencing with a conventional cell[1] and a nanopore of length 10 nm equipped with a cyclodextrin adapter give the mean residence time as $\mu_P \approx 10$ ms. (Standard deviation data are not available.) If σ_P is assumed to be ~5 ms then with the previously used data for *trans*1/*cis*2 (L_{23} = 1μm, V_{23} = 1.6 mV, $\mu_{T1} = \mu_{T2}$ = 1.6 ms, and $\sigma_{T1} = \sigma_{T2}$ = 1.3 ms) and V_{34} = 0.18 V, the value of T_{min} from Equation 38 is ~35 ms. While this is in the range of enzyme turnover rates[7] (10-80 ms), it also reduces the leeway available with sequencing design parameters. To get T_{min} below the minimum of the range for better design parameter control requires reducing the residence time of a nucleotide in the adapter either by reducing the potential difference or by altering the molecular structure of the adapter. The former has to be balanced against the resulting increase in the probability of regression of a detected base from *trans*2 into DNP.

Voltage drift

One way to solve the voltage drift problem is to use a stable reference voltage against which the drift is tracked and the difference subtracted from the recorded data (similar to the moving average in trend analysis of time series data). Alternatively the *trans*1/*cis*2 and *trans*2 compartments and DNP can be drained periodically and refilled with electrolyte. To prevent the occurrence of deletion errors due to cleaved bases still in transit through *trans*1/*cis*2 while draining is taking place, the draining step may be preceded by retraction of the strand in UNP (achieved by temporarily lowering or reversing the potential V_{05}) and pausing until the cleaved bases in transit have passed into DNP and been detected through their characteristic blockade levels. A floating electrode at the top of *trans*1/*cis*2 which is active only when retraction of the DNA strand is required may also be used for this purpose.

Accuracy with a biological DNP (AHL)

In exonuclease sequencing studies with a conventional cell[1] using AHL for DNP and an optimum potential difference of ~0.18 V over DNP the discrimination accuracy averaged over all four base types (including methylated types) is reported as 99.8%. This is based on a Gaussian fit of the data. If, however, a Voigt distribution is used the accuracy drops to 92%.[2]

S-8 OTHER TWO-PORE SYSTEMS

At least three other two-pore systems are known. One of them uses two parallel pores bridging a single *cis*-*trans* pair (with the structure [*cis*, P1-P2, *trans*]),[8] the objective being simultaneous study of two different samples. The second has been used by the company Oxford Nanopore to increase the accuracy of their strand sequencing[9] technique. Using a pair of pores (named poreA and poreK) with identical samples independently translocating through them results in a pair of non-correlated signal traces that are used to improve base calling. The third uses two pores to control the translocation of DNA.[10] A time-varying potential difference is used to ratchet the DNA back and forth through the two pores leading to current variations that are used in base identification. All three systems are materially and procedurally different from the tandem cell approach which is based on the structure [*cis* UNP *trans*/*cis* DNP *trans*] wherein a single sample goes through both pores (strand through the first, cleaved bases through the second).

REFERENCES

1 J. Clarke, H-C. Wu, L. Jayasinghe, A. Patel, S. Reid, and H. Bayley, *Nature Nanotech*., 2009, **4**, 265-270.

2 J. E. Reiner, A. Balijepalli, J. F. Robertson, D. L. Burden, B. S. Drown, and J. J. Kasianowicz, *J. Chem Phys*. 2012, **137**, 214903.

3 D. Trim, *Applied Partial Differential Equations*, Boston, PWS, 1990.

4 D. Myint-U and L. Debnath, *Linear Partial Differential Equations for Scientists and Engineers* (4th edn.), Boston, Birkhauser, 2007.

5 M. Wanunu, *Phys Life Rev*, 2012, **9**, 125–158.
6 A. B. Farimani, K. Min, and N. R. Aluru, *ACS Nano*, 2014, **8**, 7914–7922 (DOI: 10.1021/nn5029295).
7 J. H. Werner, H. Cai, R. A. Keller, and P. M. Goodwin, *Biophys. J.*, 2005, **88**, 1403–1412.
8 P. J. van der Zaag, A. van de Stolpe, E. McCoo, and E. van van Wanrooij. U. S. Pat. No. 8784632B2, July 22, 2014.
9 http://www.globalengage.co.uk/pgcasia/Brown.pdf (Accessed October 10, 2014).
10 http://twoporeguys.com/technology.html (Accessed October 10, 2014).